

# Conformationally Specific Vacuum Ultraviolet Mass-Analyzed Threshold Ionization Spectroscopy of Alkanethiols: Structure and Ionization of Conformational Isomers of Ethanethiol, Isopropanethiol, 1-Propanethiol, *tert*-Butanethiol, and 1-Butanethiol

Sunyoung Choi, Tae Yeon Kang, Kyo-Won Choi, Songhee Han, Doo-Sik Ahn, Sun Jong Baek, and Sang Kyu Kim\*

Department of Chemistry, Korea Advanced Institute of Science and Technology (KAIST) and School of Molecular Science (BK21), Daejeon (305-701), Republic of Korea

Received: February 21, 2008; Revised Manuscript Received: June 06, 2008

Conformational isomers of alkanethiols are isolated in the molecular beam, and the conformer-specific ionization dynamics have been investigated using vacuum ultraviolet mass-analyzed threshold ionization (MATI) spectroscopy. Only a single conformer of ethanethiol is observed to give the adiabatic ionization potential (IP) of  $9.2922 \pm 0.0007$  eV for the *gauche* conformer. For isopropanethiol, IP is found to be  $9.1426 \pm 0.0006$  eV for the *trans* conformer and  $9.1559 \pm 0.0006$  eV for the *gauche* conformer. Only two major conformational isomers are identified for 1-propanethiol, giving an IP of  $9.1952 \pm 0.0006$  eV for the *trans*–*gauche* conformer and  $9.2008 \pm 0.0006$  eV for the *gauche*–*gauche* conformer. The *tert*-butanethiol, as expected, has a single conformer with an IP of  $9.0294 \pm 0.0006$  eV. For 1-butanethiol, there are a number of conformers, and the assignment of the MATI bands to each conformer turns out to be nontrivial. The spectral simulation using the Franck–Condon analysis based on the density functional theory (DFT) calculations has been used for the identification of each conformational isomer in the MATI spectrum. Each conformer undergoes its unique structural change upon ionization, as revealed in the vibration resolved MATI spectrum, providing the powerful method for the spectral identification of a specific conformational isomer. The conformer specificity in the ionization-driven structural change reflects the role of the electron of the highest occupied molecular orbital (HOMO) in the conformational preference.

## Introduction

At low temperatures, molecular ensembles seek a particular three-dimensional structure, the energy of which corresponds to the global minimum in the multidimensional potential energy surfaces. However, in many molecules in which the internal rotation around the single bond has a low barrier, a number of different structures corresponding to local minima may exist.<sup>1–3</sup> At ambient conditions, those conformational isomers are all mixed together and distributed according to the Maxwell–Boltzmann statistics. Structural isomers are then subjected to chemical or biological reactions of which associated energetics and reaction pathways could be strongly dependent on the detailed molecular structures at the beginning moment of the reaction.<sup>4–7</sup> Even though it is widely accepted that the chemical and biological reactions are heavily destined by the conformational structure of the molecular system, since the isolation of the particular conformational isomer is nontrivial in many cases, the structure-based reaction mechanism has often been conjectured in explaining many important chemical reactions.

Recently, the conformer-specificity in chemical reactions has been experimentally demonstrated for several molecular systems. These include the photodissociation of the 1-iodopropane ion,<sup>8</sup> the photodissociation of the propanal ion,<sup>9</sup> the ionization-driven decarboxylation of alanine and  $\beta$ -alanine,<sup>10</sup> and the conformational control over the conical intersection dynamics of thiophenol.<sup>11</sup> These recent experimental works give promise to structure-based chemistry as an alternative tool for reaction control. For

the unambiguous tracking of a chemical reaction in a conformationally specific way, the isolation and identification of conformational isomers are essential prerequisites, especially for further conformer-specific dynamics studies. For the isolation of the conformer, one needs to cool the molecule so that the internal energy is far below the barrier along the conformational coordinate by which two or more conformational isomers are being separated. In this aspect, the supersonic jet is one of the most attractive ways of cooling, since it is so convenient and effective in getting down the internal temperature of the molecule to  $\sim 3$  K.<sup>12</sup> It is interesting to note that the supersonic

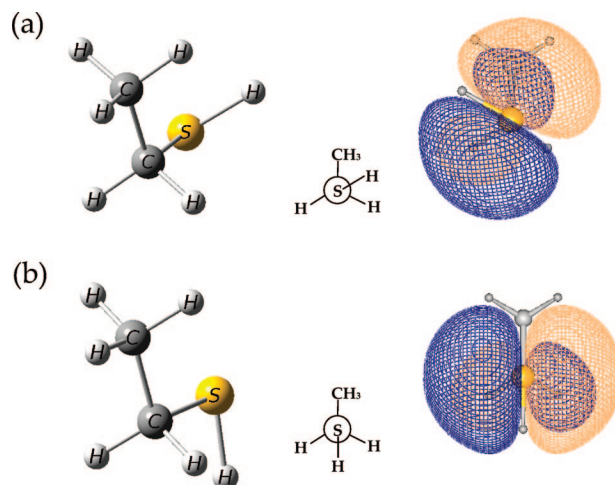


**Figure 1.** Conformational isomers of ethanethiol: (a) *gauche* and (b) *trans* isomers with their HOMOs.

\* Corresponding author. Fax: +82-42-869-2810. E-mail: sangkyukim@kaist.ac.kr.

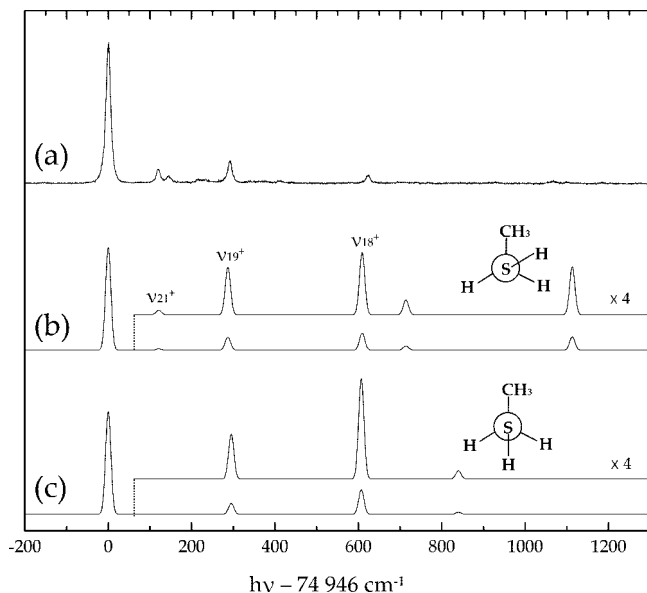


**Figure 2.** The VUV-MATI spectrum of ethanethiol (a), and the Franck-Condon simulations for (b) gauche and (c) trans using the DFT-calculated molecular geometries and vibrational frequencies (B3LYP; 6-311++G(2df, 2pd)).

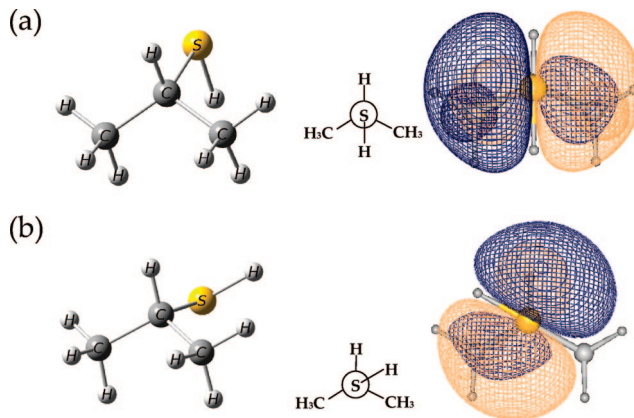
**TABLE 1: DFT-Calculated Molecular Geometries and Vibrational Frequencies of Gauche Ethanethiol (B3LYP; 6-311++G(2df, 2pd)).**

	$S_0$		$D_0$	
$R(C-S)$	1.836		1.800	
$\angle CCS$	114.45		113.00	
$\angle CSH$	97.01		98.04	
$\angle CCSH$	62.60		54.82	

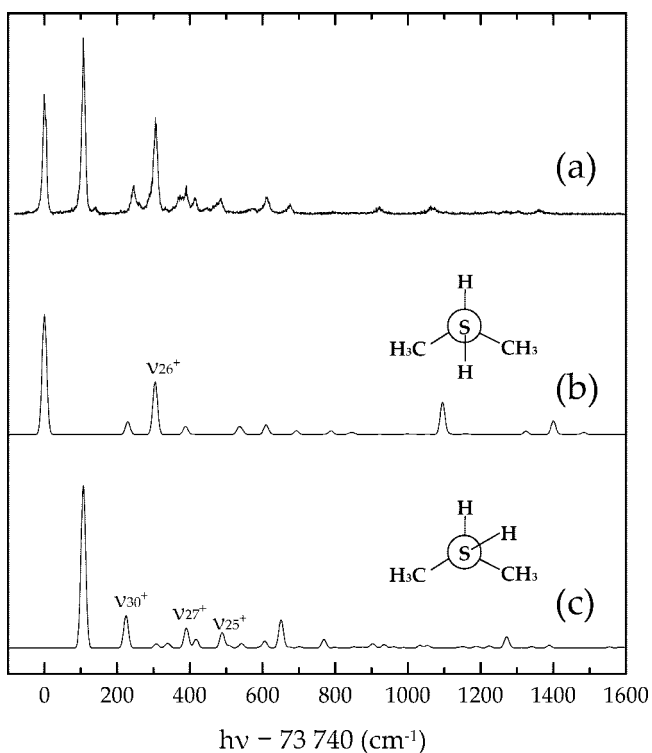
  

	$S_0$		$D_0$		
	calc	calc	calc	exp	description
$\nu_1$	3115	3146			C-H stretch
$\nu_2$	3093	3126			C-H stretch
$\nu_3$	3085	3116			C-H stretch
$\nu_4$	3057	3050			C-H stretch
$\nu_5$	3027	2980			C-H stretch
$\nu_6$	2671	2595			S-H stretch
$\nu_7$	1501	1491			CH <sub>3</sub> scissor
$\nu_8$	1493	1474			CH <sub>3</sub> deformation
$\nu_9$	1481	1424			CH <sub>3</sub> wag
$\nu_{10}$	1416	1403			CH <sub>3</sub> wag
$\nu_{11}$	1308	1299			CH <sub>2</sub> wag
$\nu_{12}$	1282	1195			CH <sub>2</sub> wag
$\nu_{13}$	1121	1113			CH <sub>2</sub> wag
$\nu_{14}$	1063	959			CH <sub>2</sub> wag
$\nu_{15}$	980	909			C-C stretch
$\nu_{16}$	876	868			CH <sub>3</sub> rock
$\nu_{17}$	737	714			CH <sub>2</sub> rock
$\nu_{18}$	647	609	623		C-S stretch
$\nu_{19}$	326	287	292		CCS bend
$\nu_{20}$	256	219			CH <sub>3</sub> torsion
$\nu_{21}$	215	121	120		SH torsion

cooling, in many cases, preserves the effective relative populations of the conformational isomers given at the temperature when the molecular sample is seeded with a carrier gas. This should originate from the fact that the supersonic cooling comes from the collisional energy transfer, and the cross section for the conformational cooling may be quite small because of the existence of the barrier among different conformers. During the internal energy minimization process, the molecule can be trapped in local minima corresponding to the nuclear configura-



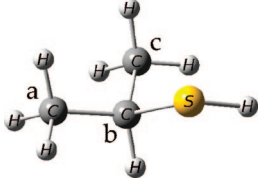
**Figure 3.** Conformational isomers of isopropanethiol: (a) trans and (b) gauche conformers with their HOMOs.



**Figure 4.** The VUV-MATI spectrum of isopropanethiol (a), with the spectral simulation for (b) trans and (c) gauche conformers using the Franck-Condon calculation based on DFT calculations (B3LYP; 6-311++G(2df, 2pd)).

tions of conformational isomers. Once the conformational isomers are isolated, one can identify each conformer through its own spectroscopic properties such as vibrational frequencies, electronic transition energies, or ionization energy. Such a spectroscopic identification would make conformer-selective chemistry possible.

In this work, vacuum ultraviolet (VUV) mass-analyzed threshold ionization (MATI) spectroscopy combined with the supersonic jet has been employed to isolate and identify the conformational isomers of several alkanethiol molecules, including ethanethiol, isopropanethiol, 1-propanethiol, *tert*-butanethiol, and 1-butanethiol. Alkanethiols are widely used as surfactants in the area of nanofabrication<sup>13</sup> and self-assembled monolayers.<sup>14,15</sup> Furthermore, conformational structures of the alkanethiol moieties of cysteine or methionine residues in proteins may play a crucial role in the folding property, leading to the structural specificity of the biological function.<sup>16,17</sup> In the cooled molecular

**TABLE 2: DFT calculated molecular geometries and vibrational frequencies of trans and gauche conformers of isopropanethiol (B3LYP; 6-311++G(2df, 2pd)).**


	trans		gauche	
	$S_0$	$D_0$	$S_0$	$D_0$
$R(C_b-S)$	1.848	1.823	1.851	1.822
$\angle C_a C_b S$	112.01	109.13	107.13	109.47
$\angle C_c C_b S$			112.12	108.10
$\angle C_a C_b C_c$	96.83	97.63	112.31	114.71
$\angle C_b S H$	112.54	113.75	97.17	98.34
$\angle H C_b S H$	180.00	180.00	63.48	52.79
$\angle H C_a C_b S$	54.34	56.67	60.04	59.45

	Trans				Gauche			
	$S_0$		$D_0$		$S_0$		$D_0$	
	calc	calc	expt	description	calc	calc	expt	description
$\nu_1$	3114	3137		C-H stretch	3106	3140		C-H stretch
$\nu_2$	3111	3135		C-H stretch	3102	3129		C-H stretch
$\nu_3$	3084	3111		C-H stretch	3092	3120		C-H stretch
$\nu_4$	3076	3106		C-H stretch	3082	3115		C-H stretch
$\nu_5$	3041	3082		C-H stretch	3052	3050		C-H stretch
$\nu_6$	3025	3036		C-H stretch	3031	3041		C-H stretch
$\nu_7$	3020	3035		C-H stretch	3021	2989		C-H stretch
$\nu_8$	2666	2603		S-H stretch	2674	2611		S-H stretch
$\nu_9$	1505	1503		CH <sub>3</sub> scissor	1508	1502		CH <sub>3</sub> scissor
$\nu_{10}$	1499	1481		CH <sub>3</sub> scissor	1499	1493		CH <sub>3</sub> deformation
$\nu_{11}$	1488	1473		CH <sub>3</sub> deformation	1489	1479		CH <sub>3</sub> scissor
$\nu_{12}$	1486	1461		CH <sub>3</sub> deformation	1486	1464		CH <sub>3</sub> deformation
$\nu_{13}$	1423	1416		CH <sub>3</sub> wag	1423	1436		CH <sub>3</sub> wag
$\nu_{14}$	1405	1399		CH <sub>3</sub> wag	1405	1400		CH <sub>3</sub> wag
$\nu_{15}$	1337	1309		CH wag	1359	1285		CH wag
$\nu_{16}$	1301	1297		CH wag	1277	1210		CH wag
$\nu_{17}$	1191	1162		CH <sub>3</sub> rock	1182	1164		CH <sub>3</sub> rock
$\nu_{18}$	1128	1096		CH <sub>3</sub> rock	1146	1117		CH <sub>3</sub> rock
$\nu_{19}$	1110	997		C-C stretch	1077	998		CH <sub>3</sub> rock
$\nu_{20}$	955	955		CH <sub>3</sub> rock	965	947		CH <sub>3</sub> rock
$\nu_{21}$	938	940		CH <sub>3</sub> rock	942	937		CH <sub>3</sub> rock
$\nu_{22}$	889	853		SH wag	899	843		SH wag
$\nu_{23}$	863	788		C-C stretch	857	795		C-C stretch
$\nu_{24}$	601	544		C-S stretch	621	544		C-S stretch
$\nu_{25}$	408	390		CCC bend	413	382	376	CCC bend
$\nu_{26}$	335	306	306	CCC bend	331	310		CCC bend
$\nu_{27}$	324	265		SH torsion	299	284	282	CCS bend
$\nu_{28}$	260	245		CH <sub>3</sub> torsion	254	228		CH <sub>3</sub> torsion
$\nu_{29}$	238	209		CH <sub>3</sub> torsion	240	201		CH <sub>3</sub> torsion
$\nu_{30}$	202	103		SH torsion	183	117	138	SH torsion

beam, several conformational isomers are isolated, and their ionization spectroscopy has been investigated. The spectral simulation using the Franck–Condon analysis based on density functional theory (DFT) calculated molecular geometries and vibrational frequencies is used for the spectral identification of conformational isomers. The structural change of each conformer upon ionization, which is revealed in the corresponding MATI spectrum, gives the information about the role of the electron in the highest occupied molecular orbital (HOMO) in retaining the nuclear layout of the preferred conformational isomer.

### Experimental Section

All chemicals were purchased (Aldrich) and used without further purification. The details of the experimental setup has

been described in our previous reports.<sup>18,19</sup> Briefly, the alkanethiol (ethanethiol, isopropanethiol, 1-propanethiol, *tert*-butanethiol, or 1-butanethiol) sample was mixed with Ar, expanded into a vacuum through a nozzle orifice (General Valve series 9) with a backing pressure of 3 atm, and skimmed through a 1 mm diameter skimmer (Precision Instrument) prior to being overlapped with a counter propagating VUV laser pulse. The tunable VUV laser pulse ( $\Delta E \sim 1 \text{ cm}^{-1}$ ,  $\Delta t \sim 5 \text{ ns}$ ) was generated via a Kr gas cell (1–2 Torr) where the four-wave mixing process occurred through the combination of the UV laser pulse fixed at 212.552 nm for the  $5p[1/2]_0-4p^6$  transition of Kr and the visible (VIS) laser pulse. A third harmonic output of a Nd:YAG laser (Continuum, Precision II) was used to pump two independently tunable dye lasers (Lambda-Physik, Scanmate 2 and Lumonics, HD-500) to generate UV and VIS laser pulses,

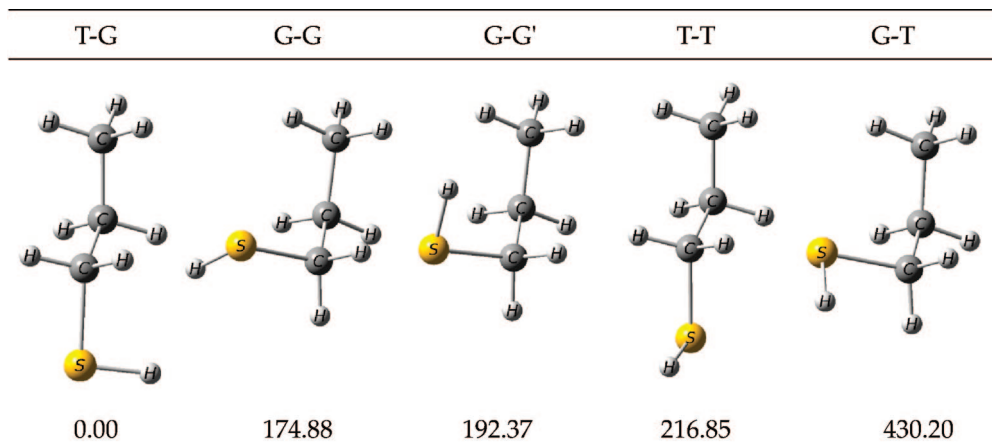


**Figure 5.** Conformational isomers of 1-propanethiol with DFT (B3LYP, 6-311++G(2df, 2pd)) calculated relative energies in  $\text{cm}^{-1}$  (zero-point energy is corrected).

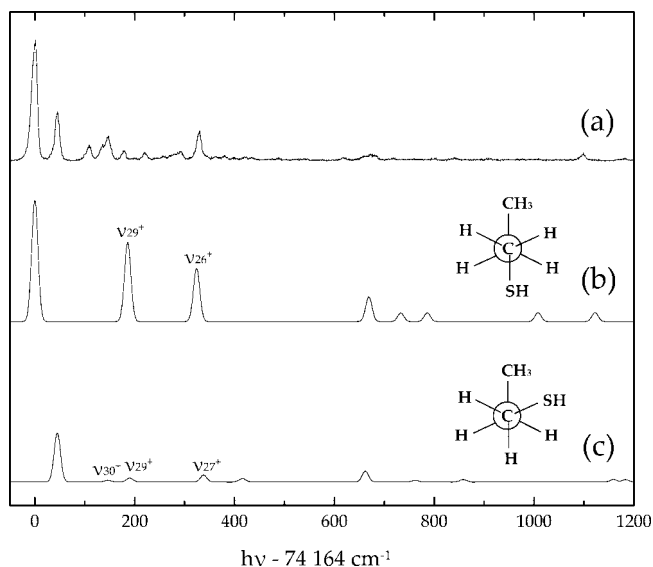
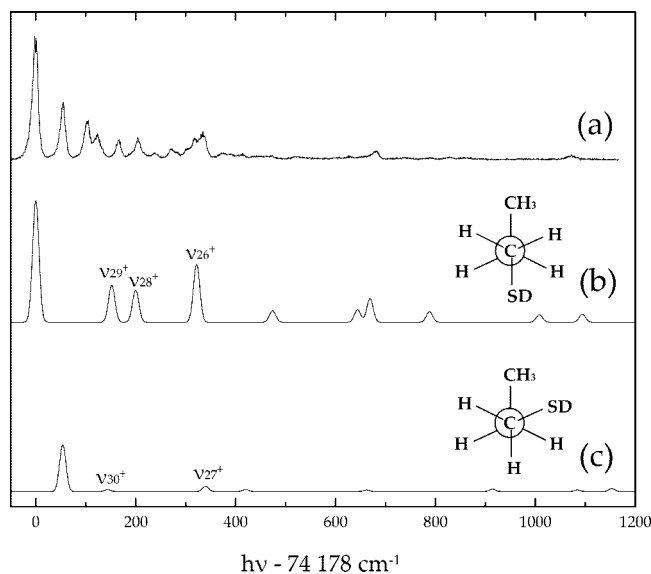


**Figure 6.** The VUV-MATI spectrum of 1-propanethiol (a), with Franck–Condon simulations for (b) trans-gauche and (c) gauche-gauche conformational isomers based on DFT calculations (B3LYP; 6-311++G(2df, 2pd)).

in which the UV was generated via the frequency doubling through a BBO crystal placed on a homemade autotracker. Molecules were directly excited to high- $n$  Rydberg states by the VUV laser pulse, and only high- $n, l$  states survived after the long delay time of 10–15  $\mu\text{s}$ . These long-lived Rydberg states were then pulsed-field ionized using a small electric field of 10 V/cm. The molecular ions were then separated according to their mass/charge ratios along the time-of-flight axis. The ion signal was digitized by an oscilloscope (LeCroy, LT584M) and monitored as a function of the VUV laser wavelength to give the corresponding MATI spectrum. All dye lasers and data-taking procedures were controlled by a personal computer. All calculations were carried out by DFT<sup>20,21</sup> with a basis set of 6-311++G(2df, 2pd) using the Gaussian 03W package.<sup>22</sup> Further exploration of the correlation consistent basis sets in the calculation was performed for the comparison. Franck–Condon analysis based on the Duschinsky transformation<sup>23</sup> was done using a code developed by Peluso and co-workers.<sup>24,25</sup>

## Results and Discussion

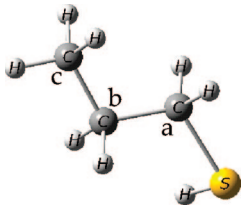
**A.. Ethanethiol.** Two conformational isomers are plausible for ethanethiol ( $\text{CH}_3\text{CH}_2\text{SH}$ ) as the internal rotation about the



**Figure 7.** (a) The VUV-MATI spectrum of the D-substituted propanethiol ( $\text{CH}_3\text{CH}_2\text{CH}_2\text{SD}$ ) and simulations for (b) TG and (c) GG conformational isomers (B3LYP; 6-311++G(2df, 2pd)).

C–S bond gives rise to two possible conformational structures of gauche and trans (Figure 1). The DFT calculation indicates that the most stable conformer is gauche, where the steric repulsion between the  $\text{CH}_3$  moiety and nonbonding orbitals mainly localized on sulfur seems to be minimized from the qualitative point of view. The calculated energy difference between energy minima of gauche and trans is  $167.9 \text{ cm}^{-1}$ . The VUV-MATI spectrum in Figure 2 indicates that there is only a single conformer in the jet, showing a strong origin peak at  $74\,946 \text{ cm}^{-1}$ , which corresponds to an adiabatic ionization energy of  $9.2922 \pm 0.0007 \text{ eV}$ , consistent with previous studies.<sup>26,27</sup> Franck–Condon analysis based on the DFT molecular structure and vibrational frequencies of gauche gives a simulated spectrum that matches the experiment quite well (Table 1 and Figure 2), confirming that the species present in the jet is the gauche conformer of ethanethiol. The spectral simulation for the trans conformer is different from that of gauche (Figure 2), indicating that the simulation method employed here is quite convincing in terms of the identification of the conformational isomer.

As indirectly known from the electron momentum spectroscopic study,<sup>28</sup> the HOMO of the neutral ground-state of ethanethiol is mainly localized on sulfur, while it has a nodal plane bisecting the C–S bond (Figure 1). Furthermore, it is

**TABLE 3: DFT Molecular Geometries and Vibrational Frequencies of the TG and GG Conformers of 1-Propanethiol (B3LYP; 6-311++G(2df, 2pd))**


	TG		GG	
	$S_0$	$D_0$	$S_0$	$D_0$
$R(S-C_a)$	1.836	1.785	1.839	1.792
$R(C_a-C_b)$	1.525	1.577	1.528	1.55
$R(C_b-C_c)$	1.530	1.532	1.527	1.526
$R(S-H)$	1.344	1.357	1.344	1.36
$\angle HSC_a$	97.05	98.49	96.87	98.02
$\angle SC_aC_b$	114.79	109.49	115.54	115.17
$\angle C_aC_bC_c$	112.24	108.07	114.42	113.30
$\angle HSC_aC_b$	63.15	73.84	67.47	53.64
$\angle SC_aC_bC_c$	177.76	175.51	65.19	66.85

$\nu$	TG-CH <sub>3</sub> CH <sub>2</sub> CH <sub>2</sub> SH				TG-CH <sub>3</sub> CH <sub>2</sub> CH <sub>2</sub> SD			
	$S_0$	$D_0$		description	$D_0$		description	
		calc	expt		calc	expt		
$\nu_1$	3099	3142		C-H stretch	3142		C-H stretch	
$\nu_2$	3093	3132		C-H stretch	3132		C-H stretch	
$\nu_3$	3084	3108		C-H stretch	3108		C-H stretch	
$\nu_4$	3057	3105		C-H stretch	3105		C-H stretch	
$\nu_5$	3050	3068		C-H stretch	3068		C-H stretch	
$\nu_6$	3027	3055		C-H stretch	3055		C-H stretch	
$\nu_7$	3026	3034		C-H stretch	3034		C-H stretch	
$\nu_8$	2666	2610		S-H stretch	1875		S-D stretch	
$\nu_9$	1510	1502		CH <sub>3</sub> + CH <sub>2</sub> scissor	1502		CH <sub>3</sub> + CH <sub>2</sub> scissor	
$\nu_{10}$	1501	1493		CH <sub>3</sub> + CH <sub>2</sub> scissor	1493		CH <sub>3</sub> + CH <sub>2</sub> scissor	
$\nu_{11}$	1494	1456		CH <sub>3</sub> deformation	1456		CH <sub>3</sub> deformation	
$\nu_{12}$	1477	1444		CH <sub>2</sub> scissor	1444		CH <sub>2</sub> scissor	
$\nu_{13}$	1415	1400		CH <sub>3</sub> wag	1400		CH <sub>3</sub> wag	
$\nu_{14}$	1369	1308		CH <sub>2</sub> wag	1308		CH <sub>2</sub> wag	
$\nu_{15}$	1325	1274		CH <sub>2</sub> twist	1274		CH <sub>2</sub> twist	
$\nu_{16}$	1282	1251		CH <sub>2</sub> wag	1243		CH <sub>2</sub> wag	
$\nu_{17}$	1254	1203		CH <sub>2</sub> wag	1203		CH <sub>2</sub> wag	
$\nu_{18}$	1132	1122		CH <sub>2</sub> twist	1094		CH <sub>2</sub> twist	
$\nu_{19}$	1099	1008		CH <sub>3</sub> wag	1008		CH <sub>3</sub> wag	
$\nu_{20}$	1032	937		C-C stretch	937		C-C stretch	
$\nu_{21}$	927	924		CH <sub>3</sub> rock	881		CH <sub>3</sub> rock	
$\nu_{22}$	898	801		CH <sub>2</sub> rock	788		C-C stretch	
$\nu_{23}$	809	786		C-C stretch	758		CH <sub>2</sub> rock	
$\nu_{24}$	735	733		CH <sub>2</sub> rock	669		C-S stretch	
$\nu_{25}$	699	669		C-S stretch	614		CH <sub>2</sub> rock	
$\nu_{26}$	359	324	329	CCC bend	322	334	CCC bend	
$\nu_{27}$	246	248		CH <sub>3</sub> torsion	248		CH <sub>3</sub> torsion	
$\nu_{28}$	231	214		SH torsion 30% + CCS bend 70%	200	205	CCS bend	
$\nu_{29}$	194	186	178	SH torsion 40% + CCS bend 60%	152	166	SD torsion	
$\nu_{30}$	113	87		C-C torsion	85		C-C torsion	

$\nu$	GG-CH <sub>3</sub> CH <sub>2</sub> CH <sub>2</sub> SH			GG-CH <sub>3</sub> CH <sub>2</sub> CH <sub>2</sub> SD		
	$S_0$	$D_0$		calc	expt	description
		calc	expt			
$\nu_1$	3105	3117		3117		C-H stretch
$\nu_2$	3100	3115		3115		C-H stretch
$\nu_3$	3088	3098		3098		C-H stretch
$\nu_4$	3057	3080		3080		C-H stretch
$\nu_5$	3039	3050		3050		C-H stretch
$\nu_6$	3029	3024		3024		C-H stretch
$\nu_7$	3010	2955		2954		C-H stretch
$\nu_8$	2673	2602		1869		S-H stretch
$\nu_9$	1510	1500		1500		CH <sub>3</sub> scissor
$\nu_{10}$	1500	1486		1486		CH <sub>2</sub> scissor
$\nu_{11}$	1487	1468		1468		CH <sub>3</sub> scissor
$\nu_{12}$	1473	1420		1420		CH <sub>3</sub> deformation

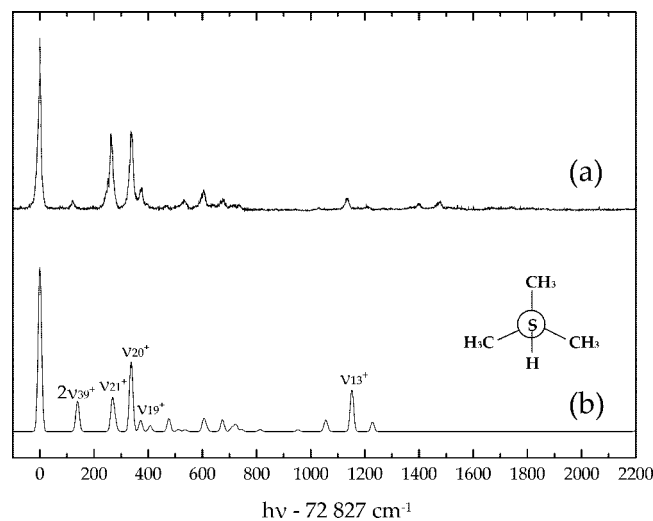
TABLE 3 Continued

	GG-CH <sub>3</sub> CH <sub>2</sub> CH <sub>2</sub> SH			GG-CH <sub>3</sub> CH <sub>2</sub> CH <sub>2</sub> SD		description
	S <sub>0</sub>	D <sub>0</sub>		D <sub>0</sub>		
		calc	expt	calc	expt	
$\nu_{13}$	1415	1406		1405		CH <sub>2</sub> scissor
$\nu_{14}$	1377	1342		1342		CH <sub>2</sub> wag
$\nu_{15}$	1330	1302		1299		CH <sub>2</sub> twist
$\nu_{16}$	1277	1260		1255		CH <sub>2</sub> twist
$\nu_{17}$	1247	1138		1131		CH <sub>2</sub> wag
$\nu_{18}$	1134	1114		1099		CH <sub>3</sub> rock
$\nu_{19}$	1076	1032		1030		CH <sub>3</sub> rock
$\nu_{20}$	1049	966		960		C–C stretch
$\nu_{21}$	935	914		860		CH <sub>2</sub> twist
$\nu_{22}$	878	813		808		C–C stretch
$\nu_{23}$	797	784		749		CH <sub>3</sub> + CH <sub>2</sub> rock
$\nu_{24}$	769	717		620		CH <sub>2</sub> rock
$\nu_{25}$	634	617		608		C–S stretch
$\nu_{26}$	423	371		366		CCC bend
$\nu_{27}$	290	293	284	286	280	CH <sub>3</sub> torsion
$\nu_{28}$	210	201		199		CH <sub>3</sub> torsion
$\nu_{29}$	200	145		121		SH torsion
$\nu_{30}$	129	101		90		C <sub>2</sub> H <sub>5</sub> torsion

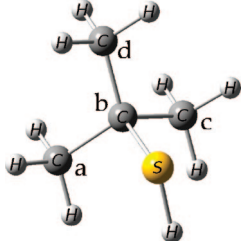
found that, from the CASSCF(3,4) calculation with a 6-31G\*\* basis set, the singly occupied molecular orbital (SOMO) of the ethanethiol cation is not only localized on sulfur, but it is also fully occupied, meaning that the multireference nature of the orbital may not be significant in this case. The structural change upon ionization should be then associated with the electron deficiency in the HOMO, even though all other occupied molecular orbitals are important for steric interactions in general. When an electron is removed from the HOMO in the *gauche* conformer, the SH torsional motion about the C–S bond is expected to be activated since the steric effect due to valence orbital repulsion should be somewhat relaxed in the ionization process, giving the associated MATI band at the vibrational energy of 120 cm<sup>-1</sup>. The nearby doublet-like feature might be due to the energy splitting caused by the conformational barrier. It should be noted that the SH torsional band is absent in the spectrum simulated for *trans* (Figure 2c), suggesting that the conformational deformation upon ionization would not be expected if the molecule in the jet were the *trans* conformational isomer. Another major change of the molecular structure upon ionization is the decrease of the C–S bond length, as reflected in the strongly observed C–S stretching band at 623 cm<sup>-1</sup> in Figure 2. The CCS bending mode is found to also be activated in the ionization with a frequency of 292 cm<sup>-1</sup>.

**B. Isopropanethiol (2-Propanethiol).** Isopropanethiol (2-propanethiol) has two different conformational isomers with respect to the torsional motion around the C–S bond. In the *trans* conformer, the SH moiety is antiparallel with the CH moiety, where the HOMO localized on sulfur is symmetric with respect to the C–S-containing plane, which bisects two methyl groups (Figure 3). Meanwhile, the SH moiety is placed on the plane more or less eclipsed with one of the methyl moieties in the *gauche* conformational isomer. The *trans* conformer is calculated to be slightly more stable than *gauche* by 10.49 cm<sup>-1</sup>, which is consistent with earlier microwave spectroscopic studies.<sup>29,30</sup> The small energy difference of two conformers explains well the almost equal population of *trans* and *gauche* conformers in the jet. Namely, two distinct origins are clearly observed with almost equal intensities in the MATI spectrum in Figure 4. The origin band at 73 740 cm<sup>-1</sup> represents the adiabatic ionization potential (IP) of the *trans* conformer, whereas the strongly observed band at 73 847 cm<sup>-1</sup> is attributed to the origin band of the *gauche* conformer ionization. This

assignment is based on the spectral simulation based on the Franck–Condon analysis using the DFT-calculated geometries and vibrational frequencies of each conformer (Figure 4 and Table 2). The simulation matches the experiment very well, making possible unambiguous assignments of the peaks belonging to individual conformational isomers, giving IP values of 9.1426 ± 0.0006 and 9.1559 ± 0.0006 eV for *trans* and *gauche* conformers of isopropanethiol, respectively. It is interesting to note that the *trans*-isopropanethiol becomes more stabilized compared to *gauche* in the cationic ground state, indicating that the charge delocalization is much more effective at the nuclear configuration of the *trans* conformer. For the *trans* conformer, the  $\nu_{26}$  mode (CCC bend) is strongly observed, whereas the  $\nu_{30}$  mode due to the SH torsional motion is found to be activated for the *gauche*-isopropanethiol. Especially, the SH torsional motion corresponds to the conformational coordinate, along which two conformational isomers are separated by a certain barrier. The conformer specificity in the ionization-driven geometrical change should originate from the three-dimensional arrangement of the HOMO of each conformer (Figure 3). In



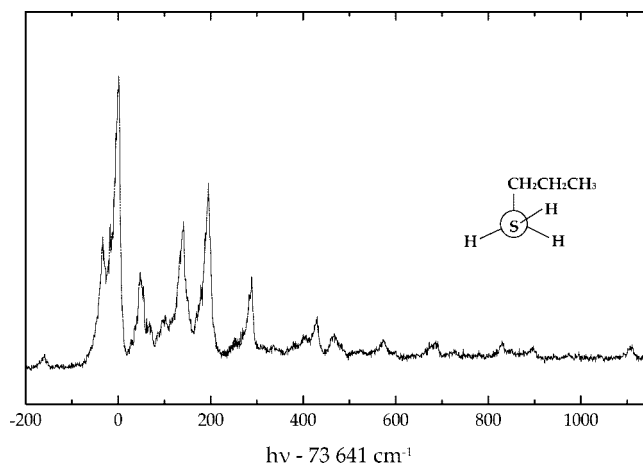
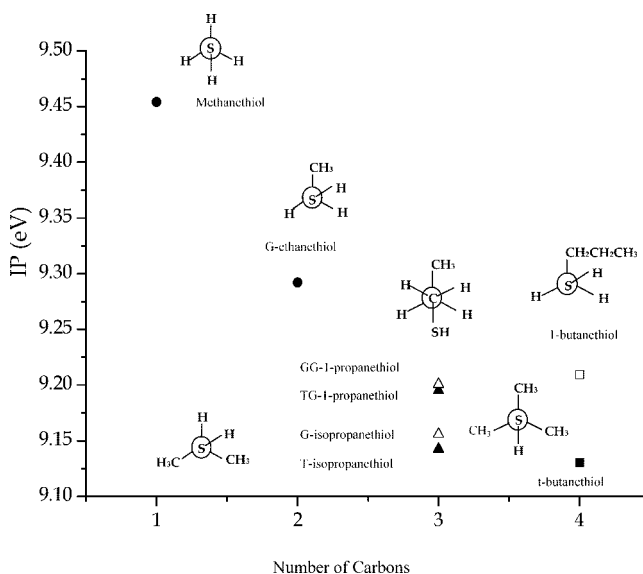
**Figure 8.** (a) The VUV-MATI spectrum of *tert*-butaneethiol and (b) Franck–Condon simulation based on DFT (B3LYP; 6-311++G(2df, 2pd)) calculated molecular geometries and vibrational frequencies (see the text).

**TABLE 4: The DFT-Calculated Molecular Geometrical Parameters and Vibrational Frequencies of *tert*-Butanethiol (B3LYP; 6-311++G(2df, 2pd))**


	$S_0$	$D_0$
$R(C_b-S)$	1.866	1.849
$R(C_b-C_d)$	1.533	1.530
$R(C_a-C_b)$	1.530	1.543
$\angle C_a C_b C_c$	110.76	111.63
$\angle C_a C_b C_d$	110.46	112.68
$\angle H S C_b$	97.07	98.19
$\angle H S C_b C_d$	180.00	180.00
$\angle H S C_b C_a$	61.12	59.63

	$S_0$	$D_0$		description
		calc	expt	
A'	$\nu_1$	3110	3131	C-H stretch
	$\nu_2$	3092	3119	C-H stretch
	$\nu_3$	3083	3103	C-H stretch
	$\nu_4$	3032	3049	C-H stretch
	$\nu_5$	3022	3030	C-H stretch
	$\nu_6$	2673	2612	S-H stretch
	$\nu_7$	1515	1513	CH <sub>2</sub> scissor
	$\nu_8$	1501	1482	CH <sub>2</sub> scissor
	$\nu_9$	1489	1474	CH <sub>2</sub> scissor
	$\nu_{10}$	1433	1441	CH <sub>3</sub> deformation
	$\nu_{11}$	1403	1405	CH <sub>3</sub> deformation
	$\nu_{12}$	1250	1228	C-C stretch
	$\nu_{13}$	1194	1152	1135 CH <sub>3</sub> rock
	$\nu_{14}$	1059	1055	1135 CH <sub>3</sub> rock
	$\nu_{15}$	939	930	1135 CH <sub>3</sub> rock
	$\nu_{16}$	872	826	HSC bend
	$\nu_{17}$	812	724	C-C stretch
$\nu_{18}$	576	493	CCC deformation	
$\nu_{19}$	391	372	373 CCC bend	
$\nu_{20}$	363	337	339 C-C stretch	
$\nu_{21}$	292	268	264 CCC deformation	
$\nu_{22}$	276	249	CH <sub>3</sub> torsion	
A''	$\nu_{23}$	3108	3130	C-H stretch
	$\nu_{24}$	3102	3125	C-H stretch
	$\nu_{25}$	3078	3100	C-H stretch
	$\nu_{26}$	3017	3031	C-H stretch
	$\nu_{27}$	1502	1497	CH <sub>2</sub> scissor
	$\nu_{28}$	1485	1480	CH <sub>2</sub> scissor
	$\nu_{29}$	1477	1458	CH <sub>2</sub> scissor
	$\nu_{30}$	1404	1398	CH <sub>3</sub> deformation
	$\nu_{31}$	1237	1184	C-C stretch
	$\nu_{32}$	1048	983	CH <sub>2</sub> rock
	$\nu_{33}$	971	950	CH <sub>2</sub> rock
	$\nu_{34}$	931	921	C-C stretch
	$\nu_{35}$	399	372	CCC bend
	$\nu_{36}$	298	274	SH + CH <sub>3</sub> torsion
	$\nu_{37}$	273	249	SH + CH <sub>3</sub> torsion
	$\nu_{38}$	241	192	CH <sub>3</sub> torsion
	$\nu_{39}$	198	70	SH torsion

other words, the HOMO, which is mainly localized on sulfur, is asymmetrically positioned with respect to the clockwise or anticlockwise torsional motion around the C-S bond in the gauche conformer. Therefore, as the electron is removed from the HOMO in the ionization process, the steric effect due to the valence orbital repulsion becomes unbalanced to induce the geometrical change along the conformational coordinate. Mean-

**Figure 9.** The VUV-MATI spectrum of 1-butanethiol. A number of conformational isomers exist in the supersonic jet. The strongest band is attributed to the origin of the most stable conformer of 1-butanethiol.**Figure 10.** The measured IPs of alkanethiols versus the number of carbons. The general trend is that IP decreases as the number of carbons increases. The IP is quite sensitive to the detailed conformational structure. The IP of only one of conformers of 1-butanethiol is plotted (see the text).

while, the HOMO of the trans conformer is symmetrically arranged with respect to the torsional motion around the C-S bond, and the electron depletion of the HOMO in trans does not cause the geometrical change along the conformational coordinate.

**C. 1-Propanethiol.** For 1-propanethiol, internal rotations about the C<sub>c</sub>-C<sub>b</sub> or C<sub>a</sub>-S bond give rise to five possible conformational isomers: trans-gauche (TG), gauche-gauche (GG), gauche-gauche' (GG'), trans-trans (TT), and gauche-trans (GT) (Figure 5). The relative stability of five conformers of 1-propanethiol seems to still be controversial, despite the number of experimental and theoretical studies in recent decades.<sup>31-40</sup> According to DFT calculations, TG is predicted to be the most stable one, whereas GG is calculated to be the second most stable conformer. In the supersonic jet, only two conformers are found to be mainly populated. Namely, in the VUV-MATI spectrum, the strong origin band is observed at 74 164 cm<sup>-1</sup>, whereas another origin band is distinctly observed at 74 209 cm<sup>-1</sup> (Figure 6). It is not unambiguous which conformers are

**TABLE 5: DFT (B3LYP) Optimized Relative ( $\text{cm}^{-1}$ ) Energies of Conformational Isomers of Ethenethiol, 1-Propanethiol, and 2-Propanethiol with Various Basis Sets<sup>a</sup>**

	cc-pVDZ	cc-pVTZ	cc-pVQZ	cc-pV5Z	6-311++G(2df, 2pd)
ethanethiol					
gauche	0	0	0	0	0
trans	253.52	179.08	172.2	174.90	182.16 (167.9)
1-propanethiol					
TG	0	0	0	0	0
GG	75.64	140.86	160.13	165.40	154.73 (174.88)
GG'	117.36	153.7	165.31	169.98	164.39 (192.37)
TT	275.77	214.45	206.97	210.30	218.16 (216.85)
GT	444.24	428.00	432.10	437.72	432.37 (430.20)
2-propanethiol					
trans	0	0	0	0	0
gauche	111.2	22.98	11.28	10.29	16.66 (10.49)

<sup>a</sup> Zero-point energy is not corrected except for the values in parentheses.

responsible for these distinct origins. The conventional way would be assigning the stronger band to the more stable conformer. However, one should also be able to explain detailed vibrational features revealed in the MATI spectrum for the proper assignment. The Franck–Condon simulation based on DFT-calculated molecular geometries and vibrational frequencies suggest that the stronger origin is attributed to the TG conformer, whereas the weaker origin is due to the GG conformer (Table 3 and Figure 6). The relative intensities of MATI bands, however, do not seem to be well explained by the Franck–Condon simulation. For instance, the simulation for the TG conformer predicts a much stronger band than the experiment for the  $\nu_{29}^+$  mode corresponding to the SH torsional motion (Figure 6b). This mismatch should come from the floppiness of 1-propanethiol. Namely, in 1-propanethiol, there exist three internal rotors, the barriers of which are very small, and the current static simulation lacks the accuracy in terms of the dynamics of the vibrational momentum in the ionization process. For confirmation of our assignment, deuterium substituted propanethiol ( $\text{CH}_3\text{CH}_2\text{CH}_2\text{SD}$ ) is investigated. Since vibrational frequencies are quite sensitive to the H–D substitution, the match between the experiment and simulation for  $\text{CH}_3\text{CH}_2\text{CH}_2\text{SD}$  strongly supports our assignment (Figure 7). It is interesting to note that the peak intensities of  $\nu_{29}^+$  and  $\nu_{28}^+$  modes for the TG conformer of  $\text{CH}_3\text{CH}_2\text{CH}_2\text{SD}$  are in good agreement with the experiment (Figure 7b). It is a bit surprising that Franck–Condon simulations for  $\text{CH}_3\text{CH}_2\text{CH}_2\text{SH}$  and  $\text{CH}_3\text{CH}_2\text{CH}_2\text{SD}$  are so different in terms of the relative intensities. It is found that, even though the geometrical parameters of  $\text{CH}_3\text{CH}_2\text{CH}_2\text{SH}$  and  $\text{CH}_3\text{CH}_2\text{CH}_2\text{SD}$  are calculated to be identical, their normal mode characters are somewhat different, especially for  $\nu_{29}^+$  and  $\nu_{28}^+$ . Namely, both the  $\nu_{28}^+$  and  $\nu_{29}^+$  modes include the significant portion of the CCS bending motion in addition to the SH torsion for  $\text{CH}_3\text{CH}_2\text{CH}_2\text{SH}$ , whereas the  $\nu_{28}^+$  and  $\nu_{29}^+$  modes of  $\text{CH}_3\text{CH}_2\text{CH}_2\text{SD}$  represent only CCS bending or SD torsion, respectively (Table 3). These normal mode calculations reflect that 1-propanethiol is so floppy that a small mass change results in the big change in the vibrational momentum of the whole molecule. Therefore, we report here that the adiabatic IP is  $9.1952 \pm 0.0006$  eV for the trans–gauche conformer and  $9.2008 \pm 0.0006$  eV for the gauche–gauche conformer of 1-propanethiol. In the supersonic jet, the population ratio of TG and GG conformers is found to be around 6 to 4. This experimental result suggests that the energy difference of TG and GG may be less than the theoretical prediction of  $175 \text{ cm}^{-1}$  (Figure 5).<sup>40</sup> Spectral simulations for other conformational isomers (GG', TT, GT) are given in the Supporting Information for the comparison.

**D. *tert*-Butanethiol and 1-Butanethiol.** Despite its large size, *tert*-butanethiol is expected to have only a single conformer, and the corresponding MATI spectrum is explained by the simulation extremely well in terms of vibrational features (Figure 8). The adiabatic IP of *tert*-butanethiol is thus determined to be  $9.0294 \pm 0.0006$  eV from the strong origin MATI band at  $72\,827 \text{ cm}^{-1}$ . Calculated geometrical parameters and vibrational frequencies are listed in Table 4. Because of the symmetry of the plane bisecting two of the three methyl moieties in the Newman projection, only the overtone of the SH torsional mode is found to be active, giving  $2\nu_{39}^+ = 121 \text{ cm}^{-1}$ . Vibrational modes of  $\nu_{20}^+$  and  $\nu_{21}^+$  corresponding to the deformation of the *tert*-butyl moiety are optically active, to give the corresponding frequencies of  $339$  and  $264 \text{ cm}^{-1}$ , respectively. These are in excellent agreement with DFT-calculated values of  $337$  and  $268 \text{ cm}^{-1}$ , respectively (Table 4). The better match of the experiment and simulation for *tert*-butanethiol compared to 1-propanethiol, despite the former's larger molecular size, should be because 1-propanethiol is much floppier than *tert*-butanethiol. A similar trend had also been observed for the MATI spectra of dimethyl sulfide (DMS) and ethylene sulfide (thiirane), where the latter shows the better match with the simulation.<sup>18</sup> For 1-butanethiol, there exist so many possible conformational isomers, and it turns out to be quite challenging to assign the MATI bands to individual conformational isomers (Figure 9). In the Supporting Information, spectral simulations for the four most stable conformers of 1-butanethiol (TG, GG', TT, GG) are given with DFT values of relative energies and vibrational frequencies. The strongest band observed at  $73\,641 \text{ cm}^{-1}$  gives an IP of  $9.1304$  eV for one of the most stable 1-butanethiol conformational isomers.

Overall, it is found that, as the alkyl chain length becomes large, the IP decreases (Figure 10). It is found that the IPs of 1-butanethiols are rather higher than the IPs of isopropanethiols and are more or less same as those of 1-propanethiols, while *tert*-butanethiol has the lowest IP among all studied here. The different conformational isomers give small but significant variations of IP. This indicates that the extent of charge delocalization through the hyperconjugation over the entire molecule is very sensitive to the detailed conformational structure. Finally, DFT calculations using several different correlation-consistent basis sets (cc-pVDZ, cc-pVTZ, cc-pVQZ, and cc-pV5Z) have been carried out for the conformational energy differences of ethanethiol, 2-propanethiol, and 1-propanethiol (Table 5). These values are compared with the DFT values calculated with a 6-311++G(2df, 2pd) basis set.



## Conclusions

In this work, conformer-specific ionization spectroscopy has been carried out for several alkanethiols, including ethanethiol, isopropanethiol, 1-propanethiol, *tert*-butanethiol, and 1-butanethiol. Using the VUV-MATI technique, the accurate IP has been determined for individual conformational isomers of each thiol compound. Unambiguous conformational assignments are successfully done through the Franck–Condon simulation of the experiment based on calculated molecular geometries and vibrational frequencies, which is quite conformer-specific. The ionization-driven structural change, revealed in the vibrational features of the MATI spectrum, is quite unique for each conformational isomer and reflects the role of the HOMO in the nuclear configuration of the associated conformer. The approach employed in this work for the identification of the conformational isomer is very promising, since low frequency vibrational modes, particularly those sensitive to the conformational nuclear arrangement, are easily accessible in the VUV-MATI spectrum. The isolation and identification of the specific conformer of thiols will allow the study of conformer-selective chemistry, where the three-dimensional molecular structure may determine the destiny of chemical reactions. By mapping out the conformer-specificity in chemical reactions, one may achieve reaction control without disentangling all the complex dynamics occurring on the multidimensional potential energy surfaces of polyatomic systems.

**Acknowledgment.** This work was financially supported by KOSEF (R01-2007-000-10766-0 & M10703000936-07M0300-93610), Echo technopia 21 project of KREST (102-071-606), Center for Space-Time Molecular Dynamics (R11-2007-012-01002-0), Korea Research Foundation (KRF-2005-070-C00063), and KISTI supercomputing center (KSC-2007-S00-1027).

**Supporting Information Available:** Franck–Condon spectral simulations for conformational isomers of 1-propanethiol (GG', TT, GT) and 1-butanethiol (TG, GG', TT, GG) are given with theoretical values for relative energies and vibrational frequencies. This material is available free of charge via the Internet at <http://pubs.acs.org>.

## References and Notes

- (1) Kurono, M.; Takasu, R.; Itoh, M. *J. Phys. Chem.* **1995**, *95*, 9668.
- (2) Finley, J. P.; Cable, J. R. *J. Phys. Chem.* **1993**, *97*, 4595.
- (3) Levy, D. H.; Wharton, L.; R.; Smalley, R. *In Chemical and Biochemical Applications of Lasers*; Moore, C. B., Ed.; Academic Press: New York, 1997; Vol. II.
- (4) Leder, L.; Berger, C.; Bornhauser, S.; Wendt, H.; Ackemann, F.; Jelesarov, I.; Bossahard, H. *Biochemistry* **1995**, *34*, 50.
- (5) Saito, S.; Shiozawa, M.; Nagahara, T.; Nakadai, M.; Yamamoto, H. *J. Am. Chem. Soc.* **2000**, *122*, 7847.
- (6) Lucero, G. C.; Woerpel, K. A. *J. Org. Chem.* **2006**, *71*, 2641.
- (7) Zuev, P. S.; Sheridan, R. S.; Sauers, R. R.; Moss, R. A.; Chu, G. *Org. Lett.* **2006**, *8*, 21.
- (8) Park, S. T.; Kim, S. K.; Kim, M. S. *Nature* **2002**, *415*, 306.
- (9) Kim, M. H.; Shen, L.; Tao, H.; Martinez, T. J.; Suits, A. G. *Science* **2007**, *315*, 1561.
- (10) Choi, K.-W.; Ahn, D.-S.; Lee, J.-H.; Kim, S. K. *Chem. Commun.* **2007**, *9*, 1041.
- (11) Lim, J. S.; Lee, Y. S.; Kim, S. K. *Angew. Chem., Int. Ed.* **2008**, *47*, 1853.
- (12) Scoles, G.; *In Atomic and Molecular Beam Methods*; Oxford University Press: Oxford, 1992; Vol. I.
- (13) Martin, C. R.; Nishizawa, M.; Jirage, K.; Kang, M.; Lee, S. B. *Adv. Mater.* **2001**, *13*, 1351.
- (14) Roy, D.; Fendler, J. *Adv. Mater.* **2004**, *16*, 479.
- (15) Burgos, P.; Geoghegan, M.; Leggett, G. J. *Nano Lett.* **2007**, *7*, 3747.
- (16) Yasui, B.; Koide, T. *J. Am. Chem. Soc.* **2003**, *125*, 15728.
- (17) Li, H.; Thomas, G. J., Jr. *J. Am. Chem. Soc.* **1991**, *113*, 456.
- (18) Choi, S.; Choi, K.-W.; Kim, S. K.; Chung, S.; Lee, S. *J. Phys. Chem. A* **2006**, *110*, 13183.
- (19) Choi, K.-W.; Ahn, D.-S.; Lee, J.-H.; Kim, S. K. *J. Phys. Chem. A* **2006**, *110*, 2634.
- (20) Becke, A. D. *J. Chem. Phys.* **1993**, *98*, 5648.
- (21) Lee, C.; Yang, W.; Parr, R. G. *Phys. Rev. B* **1988**, *37*, 785.
- (22) Frisch, M. J.; Trucks, G. W.; Schlegel, H. B.; Scuseria, G. E.; Robb, M. A.; Cheeseman, J. R.; Montgomery, J. A., Jr.; Vreven, T.; Kudin, K. N.; Burant, J. C.; Millam, J. M.; Iyengar, S. S.; Tomasi, J.; Barone, V.; Mennucci, B.; Cossi, M.; Scalmani, G.; Rega, N.; Petersson, G. A.; Nakatsuji, H.; Hada, M.; Ehara, M.; Toyota, K.; Fukuda, R.; Hasegawa, J.; Ishida, M.; Nakajima, T.; Honda, Y.; Kitao, O.; Nakai, H.; Klene, M.; Li, X.; Knox, J. E.; Hratchian, H. P.; Cross, J. B.; Bakken, V.; Adamo, C.; Jaramillo, J.; Gomperts, R.; Stratmann, R. E.; Yazyev, O.; Austin, A. J.; Cammi, R.; Pomelli, C.; Ochterski, J. W.; Ayala, P. Y.; Morokuma, K.; Voth, G. A.; Salvador, P.; Dannenberg, J. J.; Zakrzewski, V. G.; Dapprich, S.; Daniels, A. D.; Strain, M. C.; Farkas, O.; Malick, D. K.; Rabuck, A. D.; Raghavachari, K.; Foresman, J. B.; Ortiz, J. V.; Cui, Q.; Baboul, A. G.; Clifford, S.; Cioslowski, J.; Stefanov, B. B.; Liu, G.; Liashenko, A.; Piskorz, P.; Komaromi, I.; Martin, R. L.; Fox, D. J.; Keith, T.; Al-Laham, M. A.; Peng, C. Y.; Nanayakkara, A.; Challacombe, M.; Gill, P. M. W.; Johnson, B.; Chen, W.; Wong, M. W.; Gonzalez, C.; Pople, J. A. *Gaussian 03*, revision B.02; Gaussian, Inc.: Pittsburgh, PA, 2003.
- (23) Duschinsky, F. *Acta Physicochim. USSR* **1937**, *7*, 551.
- (24) Peluso, A.; Santoro, F.; Re, G. D. *Int. J. Quantum Chem.* **1997**, *63*, 233.
- (25) Borrelli, R.; Peluso, A. *J. Chem. Phys.* **2003**, *119*, 8437.
- (26) Cheung, Y.-S.; Hsu, C.-W.; Huang, J.-C.; Ng, C. Y.; Li, W.-K.; Chiu, S.-W. *Int. J. Mass. Spect. Ion. Proc.* **1996**, *159*, 13.
- (27) Cheung, Y.-S.; Huang, J.-C.; Ng, C. Y. *J. Chem. Phys.* **1998**, *109*, 1781.
- (28) Takahashi, M.; Nagasaka, H.; Udagawa, Y. *J. Phys. Chem. A* **1997**, *101*, 528.
- (29) Griffiths, J. H.; Boggs, J. E. *J. Mol. Spectrosc.* **1975**, *56*, 257.
- (30) Durlg, J. R.; Guirgis, G. A.; Compton, D. A. C. *J. Phys. Chem.* **1980**, *84*, 3547.
- (31) Pennington, R. E.; Scott, D. W.; Finke, H. L.; McCullough, J. P.; Messerly, J. F.; Hossenlopp, I. A.; Waddington, G. *J. Am. Chem. Soc.* **1956**, *78*, 3266.
- (32) Hayashi, M.; Shiro, Y.; Murata, H. *Bull. Chem. Soc. Jpn.* **1966**, *39*, 112.
- (33) Scott, D. W.; El-Sabban, Z. *J. Mol. Spectrosc.* **1969**, *30*, 317.
- (34) Torgrinnsen, T.; Klæboe, P. *Acta Chem. Scand.* **1970**, *24*, 1139.
- (35) Ogata, H.; Onizaka, H.; Nihei, Y.; Kamada, H. *Bull. Chem. Soc. Jpn.* **1973**, *46*, 3036.
- (36) Allinger, N. L.; Hickey, M. J. *J. Am. Chem. Soc.* **1975**, 5167.
- (37) Ohashi, O.; Ohnishi, M.; Tagui, A.; Sakaizumi, T.; Yamaguchi, I. *Bull. Chem. Soc. Jpn.* **1977**, *50*, 1749.
- (38) Nakagawa, J.; Hayashi, M. *J. Mol. Spectrosc.* **1981**, *85*, 327.
- (39) Li, H.; Wurrey, C. J.; Thomas, G. J., Jr. *J. Am. Chem. Soc.* **1992**, *114*, 7463.
- (40) Vansteenkiste, P.; Pauwels, E.; Speybroeck, V.; Waroquier, M. *J. Phys. Chem. A* **2005**, *109*, 9617.